

**Effect of Periodic Driving on the  
Escape in Periodic Potentials**

**Peter Jung  
Peter Hänggi**

**Report No. 9**

**1991**

**Effect of Periodic Driving on the Escape in Periodic Potentials**

**Peter Jung and Peter Hänggi**

**Lehrstuhl für Theoretische Physik, Universität Augsburg, Memminger Straße 6, D-8900 Augsburg, Germany**

*Chemical Kinetics / Diffusion / Nonequilibrium Phenomena / Statistical Mechanics*

We consider activation processes in multistable systems exposed to external fluctuations and periodic modulation. The concept of defining escape rates out of a basin of attraction as the ratio of total flux over the basin boundary and the population inside the basin of attraction is generalized for periodically driven systems. Thereby, the escape rate is connected with the Floquet-spectrum of the time inhomogeneous Fokker-Planck operator. Our formalism is demonstrated for the particular case of a multistable washboard potential. Numerical results are compared with theoretical results in the limits of small and large driving frequencies, respectively.

## 1. Introduction

Activation processes in bi- and multistable systems play an important role in many fields of physics and chemistry such as optical bistability [1], tunnel junctions [2] and chemical reaction kinetics [3] to quote but a few. The common situation is a dynamical system with at least two basins of attraction. Fluctuations provide the possibility of crossing a basin boundary and thus give rise to escape events. The statistics of barrier crossings has been discussed in terms of escape rates in the celebrated paper by Kramers [4], and subsequently in a large number of publications [5]. More recently, the role of additional periodic driving, modeling the influence of periodic external fields, has been considered in a number of experimental and theoretical investigations [6]. In the low friction regime, the dynamical system has been transformed to action angle variables, yielding under the assumption of regular deterministic motion a time homogeneous Fokker-Planck equation in action or equivalently in energy space [6a, f]. The overdamped limit has been considered recently by one of us for a quartic double well potential [7]. In the regime of small and large driving frequencies, approximation schemes have been derived [7] while, thus far, in the intermediate regime only numerical results are yet available.

In section 2 of this paper a general concept for escape rates in periodically driven systems is presented. In section 3 the particular model, Brownian motion in a washboard potential, is introduced and the equations of motion are discussed. The connections between escape rates, mobility and the diffusion coefficient in the overdamped limit are derived within a jump model in section 4. In section 5, the enhancement of the escape rate due to periodic forcing is computed as a function of the driving amplitude and frequency in the overdamped limit.

The static current voltage characteristics, i.e. the averaged velocity as a function of the bias, is known to exhibit Shapiro steps. In section 6, the dynamical current voltage characteristic, i.e. the averaged velocity as a function of the driving amplitude, is evaluated. The observed dynamical behavior is surprisingly rich and includes besides steps, which are closely related to Shapiro steps, also oscillatory behavior. One main difference to the static current-voltage characteristic is that the averaged velocity can also decrease with increasing driving amplitude.

## 2. Basic Concept

In this section a general concept for escape rates in systems with periodic forcing is presented. For the following discussion we assume that our problem is stated in terms of a set of Langevin equations

$$\dot{x}_i = h_i(x_1, x_2, \dots, x_n) + \xi_i(t) \quad i = 1, 2, \dots, n, \quad (2.1)$$

where the set  $\{x_i\}$  denotes macrovariables,  $h_i(x_1, \dots, x_n)$  are the force fields acting on  $x_i$  and  $\xi_i$  are Gaussian white noise forces, i.e.

$$\begin{aligned} \langle \xi_i(t) \rangle &= 0 \\ \langle \xi_i(t) \xi_j(t') \rangle &= 2D\delta_{ij}\delta(t-t'). \end{aligned} \quad (2.2)$$

The dynamical system without noise is assumed to have two coexisting basins of attraction,  $A_1$  and  $A_2$ . Under the influence of noise, the systems can cross the basin boundary and can thus escape from one basin of attraction to the other. Injecting particles in  $A_1$  and absorbing them in the neighboring attractor  $A_2$  (by appropriate use of reflecting and absorbing boundary conditions [3]) a stationary flux  $S_{12}(x)$  over the basin boundary  $\partial(A_1, A_2)$  between  $A_1$  and  $A_2$  builds up. The escape rate from  $A_1$  to  $A_2$  is then given by the ratio of the total flux over the basin boundary and the total population in  $A_1$ , i.e. [8]

$$r^{12} = \frac{\int_{\partial(A_1, A_2)} dx^{n-1} n(x) S_{12}(x)}{\int_{A_1} dx^n p(x)}. \quad (2.3)$$

In the weak noise limit, i.e.  $D \rightarrow 0$ , the rates are connected to the smallest non-vanishing eigenvalue  $\lambda_{\min}$  of the Fokker-Planck equation, corresponding to (2.1, 2.2), by

$$\lambda_{\min} = r^{12} + r^{21}. \quad (2.4)$$

In periodically driven systems, e.g.

$$\begin{aligned} \dot{x}_i &= h_i(x_1, x_2, \dots, x_n) + \delta_{ik} A \sin \Omega t + \zeta_i(t), \\ i &= 1, 2, \dots, n \text{ and } k \in [1, n], \end{aligned} \quad (2.5)$$

there is no stationary structure of attractors in the phase space, spanned up by the variables  $x_i$ . Thus, the flux-over-population method cannot immediately be applied. Time dependent escape rates, defined as momentary rates have been discussed in the literature [9]. As a consequence, the decay of the population is non-exponential [10]. The latter conception is therefore questionable. In the following we introduce a concept which results in time independent escape rates and in exponentially decaying populations.

In a first step we extend the phase space to  $n+1$  dimensions by introducing the additional variable  $\Theta \equiv \Omega t + \varphi$ . Escape rates are now defined in the same way just as in the stationary case, but now in the extended phase space. Particles have to be injected into and absorbed out of the relevant attractors in the extended phase space. The resulting stationary flux has to be integrated along the basin boundary of the extended phase space. Since the integration of the flux along the basin boundary involves also an integration over the additional variable  $\Theta$ , the total flux and thus also the rate is time-independent [7, 11]. The smallest non-vanishing eigenvalue  $\lambda_{\min}^{(2)}$  of the Fokker-Planck equation in the extended phase space is connected in the limit of weak noise to the escape rates  $r^{12}$  and  $r^{21}$  evaluated via flux over population method in the extended phase space by

$$\lambda_{\min}^{(2)} = r^{12} + r^{21}. \quad (2.6)$$

The eigenvalues of the Fokker-Planck equation in the extended phase space are identical with the Floquet-coefficients of the non-stationary stochastic process in  $n$  dimensions [7, 11, 12] (described by the Fokker-Planck equation corresponding to (2.1) without extending the phase space),

Thus, the escape rate of the periodically driven stochastic process (2.5) is also given by the smallest non-vanishing Floquet-coefficient of the corresponding time inhomogeneous Fokker-Planck equation.

In one dimensional bistable systems, i.e.  $n = 1$ , the extended phase space is the two-dimensional  $x - \Theta$ -space. The basin boundary is the unstable periodic orbit, i.e.  $\partial(A_1, A_2)$  is a one-dimensional object in  $x - \theta$ -space. In two-dimensional problems, such as the Kramers' problem with periodic driving,  $\dot{x} = v$ ,  $\dot{v} = -\gamma v + f(x) + A \sin \Omega t + \zeta(t)$ , the extended phase space becomes three-dimensional and the basin boundary is an object which is two dimensional below homoclinic threshold (regular motion), and a fractal above homoclinic threshold (irregular motion). The escape in the latter case is connected with the flux through a fractal basin boundary. While the regular regime has been treated in the weak damping limit within an energy diffusion equation as mentioned in the introduction, the irregular regime is not yet solved.

### 3. The Model: Equations of Motion

The (tilted) one dimensional washboard potential

$$V(x) = -d \cos x - \hat{F}x \tag{3.1}$$

is a multistable potential for  $\hat{F} < d$  with minima and maxima given by

$$x_{\pm}^{\text{min}} = \arcsin \frac{\hat{F}}{d} + 2\pi n \quad n = 0, \pm 1, \pm 2, \dots \tag{3.2}$$

$$x_{\pm}^{\text{max}} = \pi - \arcsin \frac{\hat{F}}{d} + 2\pi n \quad n = 0, \pm 1, \pm 2, \dots \tag{3.3}$$

The variable  $x$  is dimensionless and can thus be interpreted as an angle variable (but not necessarily modulo  $2\pi$ ). The Newtonian equation of motion supplemented by a noise term, i.e. the Langevin equation, reads:

$$\ddot{x} + \dot{\gamma} \dot{x} - V'(x) = \hat{A} \sin(\omega \hat{t}) + \zeta(\hat{t}), \tag{3.4}$$

where dots indicate differentiation with respect to the time  $\hat{t}$ . The fluctuation-dissipation-theorem of the second kind [13] is fulfilled without periodic driving, i.e.

$$\langle \zeta(\hat{t}) \zeta(\hat{t}') \rangle = 2\dot{\gamma} k T \delta(\hat{t} - \hat{t}'). \tag{3.5}$$

In dimensionless variables, i.e.

$$\begin{aligned} \bar{t} &\equiv \sqrt{d} \hat{t} \\ \gamma &\equiv \dot{\gamma} / \sqrt{d} \\ A &\equiv \hat{A} / \sqrt{d} \\ \bar{\Omega} &\equiv \omega / \sqrt{d} \\ D &\equiv kT/d \\ F &\equiv \hat{F}/d \end{aligned}$$

the Langevin equation (3.4) reads

$$\ddot{x} + \gamma \dot{x} + \sin x = F + A \sin(\bar{\Omega} \bar{t}) + \zeta(\bar{t}) \tag{3.6}$$

with

$$\langle \zeta(\bar{t}) \zeta(\bar{t}') \rangle = 2\dot{\gamma} D \delta(\bar{t} - \bar{t}'). \tag{3.7}$$

Here, the dots denote differentiation with respect to  $\bar{t}$ . For large damping, i.e.  $\gamma \gg \sqrt{d}$ , the first term on the l.h.s. of (3.6) or equivalently (3.4) can be neglected, and we obtain

$$\frac{dx}{dt} = -\sin x + F + A \sin \Omega t + \sqrt{D} \zeta(t), \tag{3.8}$$

with the scaled time  $t \equiv (d/\dot{\gamma}) \bar{t} = \gamma^{-1} \bar{t}$  and the scaled frequency  $\Omega = \dot{\gamma} \bar{\Omega} = (\dot{\gamma}/d) \omega$ .

### 4. Escape Rates, Mobility and Diffusion Constant in the Overdamped Limit

The stochastic dynamics in the multiwell potential (3.1) may be modelled by a hopping dynamics between the wells. In the overdamped case there is only hopping between neighboring wells, i.e.

$$\dot{P}_n = r^+ P_{n-1} + r^- P_{n+1} - (r^+ + r^-) P_n, \tag{4.1}$$

where  $P_n$  denotes the probability that the system is in the  $n$ -th well and  $r^\pm$  are the escape rates from the  $n$ -th to the  $(n \pm 1)$ -th well. The rates  $r^+$  and  $r^-$  are assumed to be independent of the site  $n$ . In periodically modulated systems the rates and populations above are understood as those defined in the extended phase space. The stationary solution for  $k$ -fold periodic boundary conditions, i.e.

$$P_{n+2\pi k} = P_n \tag{4.2}$$

is the uniform distribution

$$P_n^{(st)} = 1/k. \tag{4.3}$$

The mean velocity is given by the product of the stationary flux  $(r^+ - r^-) P_n^{(st)}$  and the length  $2\pi k$ , i.e.

$$\langle v \rangle = 2\pi(r^+ - r^-). \tag{4.4a}$$

The mobility, defined by the ratio of the mean velocity  $\langle v \rangle$  and force  $F$  then reads

$$\mu = \frac{\langle v \rangle}{F} = \frac{2\pi}{F} (r^+ - r^-). \tag{4.4b}$$

The diffusion coefficient can be obtained from the first and second-order moments  $\langle n(t) \rangle$  and  $\langle n^2(t) \rangle$  of the master equation (4.1)

$$\begin{aligned} \langle n^2(t) \rangle &= (r^+ + r^-) t + (r^+ - r^-)^2 t^2 \\ \langle n(t) \rangle &= (r^+ - r^-) t. \end{aligned} \tag{4.5}$$

The second term on the r.h.s. of the first equation of (4.5) is a transport term and vanishes for zero bias, while the first term on the r.h.s. of (4.5) is a diffusive term. The diffusion coefficient  $D_{\text{eff}}$ , defined by

$$D_{\text{eff}} = \frac{1}{2} \frac{d}{dt} \langle (x(t) - \langle x(t) \rangle)^2 \rangle \quad (4.6)$$

is given by

$$D_{\text{eff}} = \frac{1}{2} (2\pi)^2 \frac{d}{dt} (\langle n^2(t) \rangle - \langle n(t) \rangle^2) = 2\pi^2 (r^+ + r^-). \quad (4.7)$$

In the weak noise limit, the escape rate is connected with the smallest non-vanishing eigenvalue of the Fokker-Planck operator corresponding to (3.3) in the extended phase space.

A delicate problem, however, is the choice of the boundary conditions for the Fokker-Planck equation. Using simple periodic boundary conditions, i.e.  $P(x, \theta, t) = P(x + 2\pi, \theta, t)$ , the potential is not bistable in the interval  $[0, 2\pi]$ . The outgoing flux at one boundary is identical with the incoming flux at the other boundary. Thus, the population in the well is not decaying and the smallest non-vanishing eigenvalue has not the meaning of an escape rate. Using two-fold periodic boundary conditions, i.e.  $P(x, \theta, t) = P(x + 4\pi, \theta, t)$ , the potential is bistable in  $[0, 4\pi]$ . Thus, the population in one of the wells may decay, and the smallest non-vanishing eigenvalue  $\lambda_{\text{min}}$  is connected with the escape rates  $r^\pm$  by

$$\lambda_{\text{min}} = 2(r^+ + r^-). \quad (4.8)$$

Using  $n$ -fold periodic boundary conditions, i.e.  $P(x, \theta, t) = P(x + 2\pi n, \theta, t)$ , additional branches of eigenvalues emerge, being connected with relaxation processes between not-adjacent potential wells. The situation can be understood in terms of a Bloch theory. A periodic force field in space  $x$  provides eigen-solutions of the Bloch-type,

$$\psi_\sigma^k(x, \theta) = \exp(ikx) u_\sigma^k(x, \theta) \quad (4.9a)$$

with

$$u_\sigma^k(x + 2\pi, \theta) = u_\sigma^k(x, \theta), \quad (4.9b)$$

where the quasi continuous index  $k$  may be restricted to the first Brillouin zone (Bz), i.e.  $-1/2 < k < 1/2$  (in the symmetric choice). In Fig. 1 a typical band structure is sketched for illustration. The other index  $\sigma$  numbers the eigenvalues for a given value of  $k$ , i.e. is the analogue to the band index in solid state theory. Simple periodic boundary conditions restrict the possible values for  $k$  to  $k=0$ , while two-fold periodic boundary conditions allow for  $k=0, \pm 1/2$ .  $n$ -fold periodic boundary conditions select as possible values  $k_n = 0, \pm 1/n, \pm 2/n, \dots$  with  $|k_n| < 1/2$ . The relevant eigenvalue for the rate, however, is only the smallest non-vanishing eigenvalue at one of the boundaries of the first Bz, although there are smaller eigenvalues within the first Bz.

Note, that for  $(2n+1)$ -fold periodic boundary conditions, the Bz boundaries  $k = \pm 1/2$  are not allowed values. Therefore, for this choice of boundary conditions the rates are not connected via (4.8) to eigenvalues!

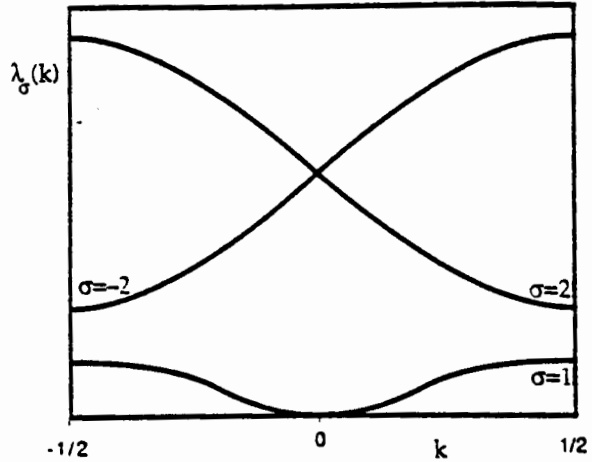


Fig. 1

A typical reduced band structure for the eigenvalues of a Fokker-Planck equation with a periodic potential is shown. Two bands  $\sigma=1$  and  $\sigma=\pm 2$  are plotted within the first Brillouin zone  $k \in [-1/2, 1/2]$ .

The individual rates  $r^\pm$  may be obtained by using (4.4b) and (4.3), i.e.

$$r^\pm = \frac{\lambda_{\text{min}}}{4} \pm \frac{\mu F}{4\pi}. \quad (4.10)$$

For symmetric potentials ( $F=0$ ) the rates  $r^\pm$  are obtained from the eigenvalue  $\lambda_{\text{min}}$  only, while for tilted potentials ( $F \neq 0$ ) it is necessary to compute also the mobility.

Finally we note that the diffusion coefficient  $D_{\text{eff}}$  in (4.6) is connected to the eigenvalue  $\lambda_{\text{min}}$  by

$$D_{\text{eff}} = \pi^2 \lambda_{\text{min}}. \quad (4.11)$$

#### 4.1. Results for the Unperturbed System ( $A=0$ )

Here we briefly review on the results without periodic driving. In Gaussian approximation the rates are given by [14]

$$r^\pm = \frac{1}{2\pi} \sqrt{1-F^2} \exp \left[ -\frac{1}{D} (\mp F + 2F \arcsin F + 2\sqrt{1-F^2}) \right]. \quad (4.12)$$

The total rate out of a potential well is then given by

$$\begin{aligned} r_0 &= r^+ + r^- \\ &= \frac{1}{\pi} \sqrt{1-F^2} \exp \left[ -\frac{2}{D} F \arcsin F \right. \\ &\quad \left. - \frac{2}{D} \sqrt{1-F^2} \right] \cosh \left( \frac{F\pi}{D} \right). \end{aligned} \quad (4.13)$$

In (4.12) and (4.13) the normalization of (3.8) has been used. The mobility is obtained from (4.4b), i.e.

$$\mu = \frac{2}{F} \sqrt{1-F^2} \exp \left[ -\frac{2}{D} F \arcsin F - \frac{2}{D} \sqrt{1-F^2} \right] \sinh \left( \frac{F\pi}{D} \right), \quad (4.14)$$

while the diffusion coefficient  $D_{\text{eff}}$  is given by

$$D_{\text{eff}} = 2\pi \sqrt{1-F^2} \exp \left[ -\frac{2}{D} F \arcsin F - \frac{2}{D} \sqrt{1-F^2} \right] \cosh \left( \frac{F\pi}{D} \right). \quad (4.15)$$

**5. Escape Rates for the Periodically Forced System in the Overdamped Limit**

The Langevin equation (3.8) in the extended phase space reads

$$\begin{aligned} \dot{x} &= -\sin x + F + A \sin \theta + \zeta(t) \\ \dot{\theta} &= \Omega. \end{aligned} \quad (5.1)$$

Without noise, the unstable periodic orbits for small  $A/\Omega^2$  may be obtained by linearization around the unstable fixed points, i.e.

$$x_{\text{un}}^{\pm}(\theta) = \pi(2n+1) - \arcsin F + \frac{A}{\sqrt{1-F^2+\Omega^2}} \sin \left[ \theta - \arctan \left( \frac{\Omega}{\sqrt{1-F^2}} \right) \right], \quad (5.2)$$

where  $n = 0, \pm 1, \pm 2, \dots$ . The stable periodic orbits for small  $A/\Omega^2$  are obtained similarly and are given by

$$x_{\text{st}}^{\pm}(\theta) = 2n\pi + \arcsin F + \frac{A}{\sqrt{1-F^2+\Omega^2}} \sin \left( \theta - \arctan \left( \frac{\Omega}{\sqrt{1-F^2}} \right) \right). \quad (5.3)$$

In Fig. 2, the  $x-\theta$  phase space ( $x \in [-\pi, 3\pi]$ ,  $\theta \in [0, 2\pi]$ ) is shown with numerically evaluated stable and unstable periodic orbits without bias ( $F=0$ ) for  $A=0.5$ . The unstable periodic orbit divides the phase space into two basins of attraction. The basin boundary becomes for large frequencies  $\Omega$  or small driving amplitudes  $A$  a straight line. The escape rate is given in terms of the smallest non-vanishing real eigenvalue  $\lambda_{\text{min}}(A, \Omega, D)$  of the Fokker-Planck equation

$$\begin{aligned} \frac{\partial}{\partial t} P(x, \theta, t) &= \frac{\partial}{\partial x} (\sin x + A \sin \theta) P(x, \theta, t) \\ &\quad - \Omega \frac{\partial}{\partial \theta} P(x, \theta, t) + D \frac{\partial^2}{\partial x^2} P(x, \theta, t) \\ &\equiv L_{\text{FP}} P(x, \theta, t) \end{aligned} \quad (5.4)$$

for periodic boundary conditions in  $\theta$ , i.e.  $P(x, \theta, t) = P(x, \theta + 2\pi, t)$  and two-fold periodic boundary conditions in  $x$ , i.e.  $P(x, \theta, t) = P(x + 4\pi, \theta, t)$ . More generally, the full band-scheme for the eigenvalues  $\lambda_{\sigma}(k)$  is obtained from the boundary value problem

$$\begin{aligned} [\lambda_{\sigma}(k) + Dk^2] u_{\sigma}^k(x, \theta) &= \left[ L_{\text{FP}} + ik(\sin x + A \sin \theta) \right. \\ &\quad \left. + 2iDk \frac{\partial}{\partial x} \right] u_{\sigma}^k(x, \theta) \end{aligned} \quad (5.5)$$

with simple periodic boundary conditions for  $u_{\sigma}^k(x, \theta)$  in  $\theta$  and  $x$  and  $k \in [-1/2, 1/2]$ . As already mentioned earlier,  $\lambda_{\text{min}}$  is identical with  $\lambda_{\sigma=1}(k=1/2)$ .

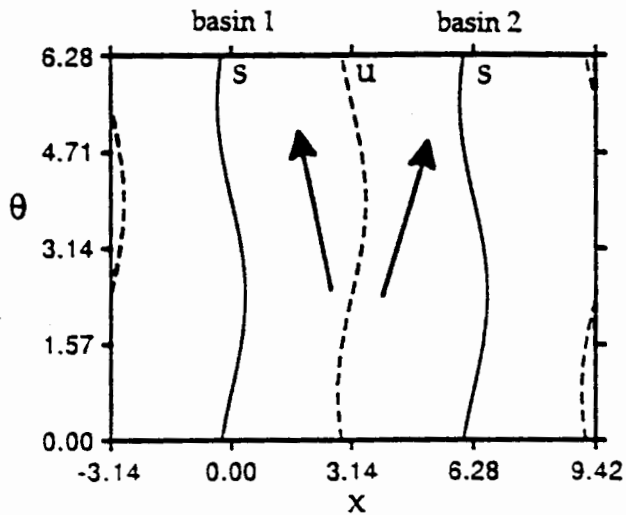


Fig. 2 The stable (full lines) and unstable (dashed lines) periodic orbits are shown in the  $x-\theta$  phase space. The unstable periodic orbit close to  $x = \pi$  separates the phase space  $x \in [-\pi, 3\pi]$  into two basins of attraction. The attractors are the stable periodic orbits (limit cycles) in the  $x-\theta$  phase space

The numerically evaluated rate enhancement  $\eta(A, \Omega, D)$  due to the periodic driving, i.e.

$$\eta(A, \Omega, D) = \frac{\lambda(A, \Omega, D)}{\lambda(A=0, D)} - 1 \quad (5.6)$$

is plotted in Fig. 3 as a function of the amplitude  $A$  for different values of the driving frequency in a double logarithmic plot. The straight lines for small  $A$  with a slope of 2 clearly indicate the law

$$\eta(A, \Omega, D) = \kappa(\Omega, D) A^2 \quad (5.7)$$

being valid for small driving amplitudes  $A$ . In Fig. 4, the rate enhancement factor  $\kappa(\Omega, D)$  is shown as a function of the driving frequency  $\Omega$  for various values of the noise strength  $D$  in a double logarithmic plot. For small  $\Omega$ , the factor  $\kappa$  reaches a certain plateau, while for large  $\Omega$  the rate enhancement factor exhibits a decrease  $\propto \Omega^{-2}$ .

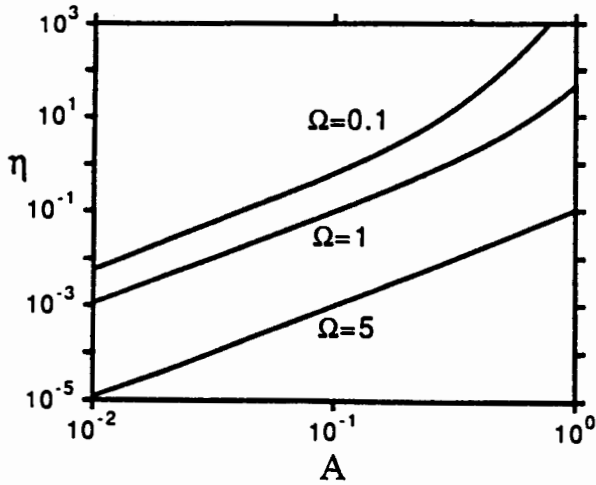


Fig. 3  
The rate enhancement  $\eta(A, \Omega)$  is shown as a function of  $A$  in a double logarithmic plot for  $\Omega = 0.1$ ,  $\Omega = 1$  and  $\Omega = 5$ . The power law for small  $A$  is evident

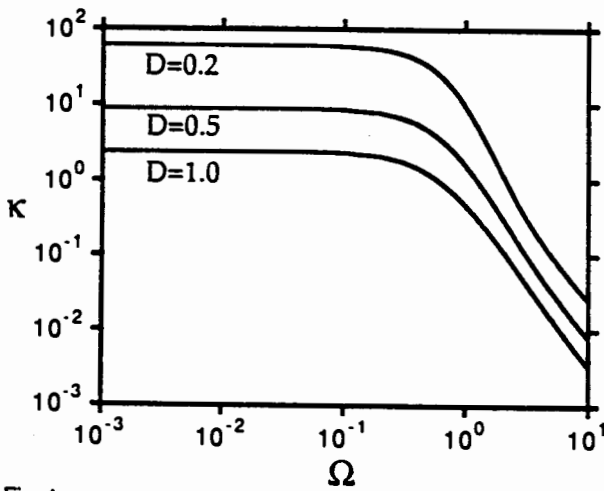


Fig. 4  
The rate enhancement factor  $\kappa$  is shown as a function of the driving frequency  $\Omega$  for  $D = 0.2$ ,  $D = 0.5$  and  $D = 1$

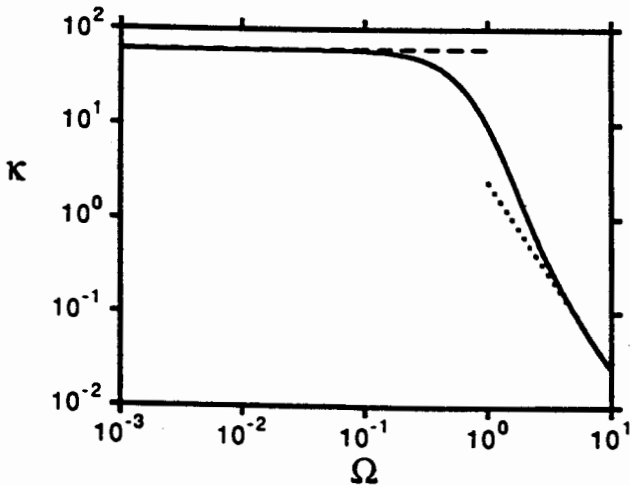


Fig. 5  
The rate enhancement factor  $\kappa$  is compared with the theoretical results (5.9) and (5.10) at  $D = 0.2$  for small and large driving frequencies.

Both limits,  $\Omega$  small and  $\Omega$  large, can be described approximately. For small frequencies  $\Omega \ll \omega_{\text{hopping}}$  an adiabatic approximation [7] yields

$$\eta(A, \Omega, D) \approx I_0(A\pi/D) - 1, \quad (5.8)$$

where  $I_0(x)$  is a modified Bessel function [15]. For  $A/D \rightarrow 0$  one finds approximately

$$\kappa(\Omega, D) = \frac{\eta}{A^2} \approx \frac{\pi^2}{4D^2}. \quad (5.9)$$

The crux with the adiabatic approximation is that with small noise strength it is valid only for exponentially small driving frequencies.

In the high frequency limit the averaging method of Ref. 7 yields for the rate enhancement

$$\eta(A, \Omega, D) \approx \frac{1}{2D\Omega^2} A^2 \text{ or } \kappa \approx \frac{1}{2D\Omega^2}. \quad (5.10)$$

Both limits (5.9) and (5.10) are compared with the numerical results for  $D = 0.2$  in Fig. 5.

We do not discuss individual rate  $r^+$  or  $r^-$  in the presence of bias ( $F \neq 0$ ), since the effect of periodic driving is the same as in the symmetric case ( $F = 0$ ). We want to point out, however, that they can be obtained by computing the averaged mobility  $\mu$  and the relevant eigenvalue  $\lambda_{\text{min}}$  and by using (4.10). The effective diffusion coefficient  $D_{\text{eff}}$  (4.6) is connected with the relevant eigenvalue  $\lambda_{\text{min}}$  by Eq. (4.11) and thus exhibits the same dependence on the driving frequency and amplitude.

## 6. The Dynamical Current-Voltage Characteristic

The current-voltage characteristics of the model (3.8), i.e.  $\langle \dot{x} \rangle$  ( $\equiv$  voltage) as a function of the bias  $F$  ( $\equiv$  current) has been discussed in the context of Josephson junctions [16], phase locking in electric circuits [17] and mode locking in ring laser gyroscopes [18]. The periodic driving gives rise to steps which have been observed first by Shapiro [19] in Josephson junctions. In terms of the model (3.8) without noise, these steps occur when the periodic output  $x_p(t)$  "locks" into the phase of the periodic driving. The locking condition is fulfilled when the period  $T = 2\pi/\Omega$  of the driving is a multiple of the time  $T_s$  the system needs for running down the tilted potential one period  $L = 2\pi$ , i.e. when

$$\langle \dot{x} \rangle = n\Omega, \quad (6.1)$$

where  $\langle \dot{x} \rangle$  is the averaged velocity along one spatial period  $2\pi$ . The influence of noise consists in rounding the steps or destroying them if the noise strength is sufficiently large. Characteristic is the stepwise but monotonous increase of the voltage with increasing current  $F$ .

The dynamical current-voltage characteristic will be defined as the voltage  $\langle \dot{x} \rangle$  as a function of the driving amplitude  $A$ . Without noise, such a dynamical current-voltage

characteristic is shown in Fig. 6a for  $F=0.8$  and  $\Omega=1$  (dashed line). The voltage vanishes for  $A < A^{(1)}$ , since the system cannot overcome the barrier. At  $A = A^{(1)}$  the system jumps into a running state, and is locked into the phase of the periodic driving in the locking regime  $n=1$  (see Eq. (6.1)). For  $A^{(3)} > A > A^{(2)}$  the locking conditions cannot be fulfilled (for an explanation see below) and the voltage drops down. The locking conditions are fulfilled only on disconnected intervals of the  $A$ -axis, and the width of the locked regions decreases for increasing driving amplitudes  $A$ . For very large values of  $A$ , i.e.  $A \rightarrow \infty$ , the locking condition cannot be fulfilled any more and the voltage relaxes oscillatory to its asymptotic value  $\langle \dot{x} \rangle = F$ . The influence of noise (full line in Fig. 6a) results in rounding off the plateaus in the phase locked regions and finally in destroying the phase locking for large driving amplitudes.

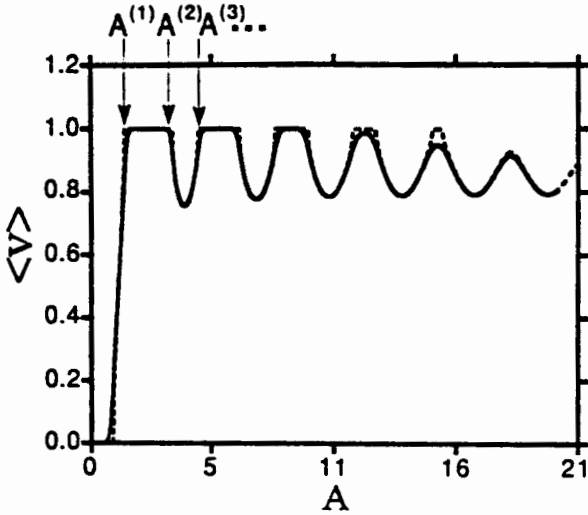


Fig. 6a: The dynamical current-voltage characteristic ( $\langle \dot{v} \rangle \equiv \langle \dot{x} \rangle$ ) is shown for  $F=0.8$  and  $\Omega=1$  without noise (dashed line) and with the noise strength  $D=0.01$  (full line)

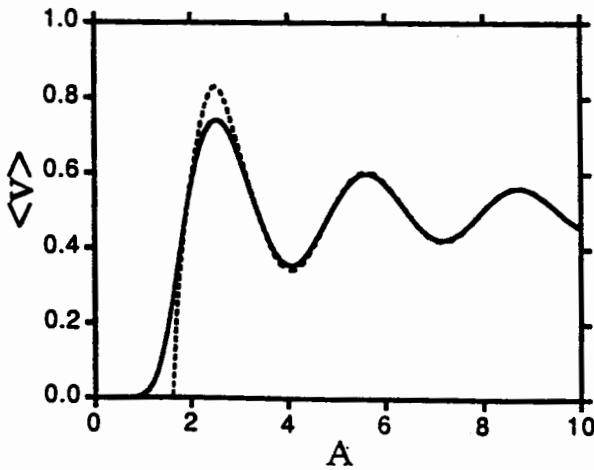


Fig. 6b: The dynamical current-voltage characteristic ( $\langle \dot{v} \rangle \equiv \langle \dot{x} \rangle$ ) is shown for  $F=0.5$  and  $\Omega=1$  without noise (dashed line) and with the noise strength  $D=0.01$  (full line).

In Fig. 6b the dynamical current voltage characteristics is shown for the smaller bias  $F=0.5$ . Here are no phase locked regions at all. The locked regions are estimated without noise in the following [20]. For convenience we choose a cos-driving in the equation of motion, i.e.

$$\dot{x} = -\sin x + A \cos \Omega t + F. \tag{6.2}$$

Inserting the ansatz

$$x(t) = x_0 + \frac{A}{\Omega} \sin \Omega t + \langle \dot{x} \rangle t \tag{6.3}$$

into (6.2) we obtain

$$\langle \dot{x} \rangle = F - \sum_{k=-\infty}^{\infty} J_k(A/\Omega) \sin(x_0 + (k\Omega + \langle \dot{x} \rangle)t) \tag{6.4}$$

from which  $\langle \dot{x} \rangle$  follows self consistently. In (6.4)  $J_k(x)$  are Bessel functions [15], and  $x_0$  is an arbitrary phase. In the phase locked regions we find by using (6.1) and averaging over one period the conditions for locking into the  $n$ -th region, i.e.

$$F - n\Omega = J_n(A/\Omega) (-1)^n \sin x_0. \tag{6.5}$$

For the 0-th region ( $\langle \dot{x} \rangle = 0$ ) the condition  $F = J_0(A/\Omega) \sin x_0$  has to be fulfilled. The solution is discussed graphically in Fig. 7 for  $F=0.8$ . It follows from Fig. 7 that for  $A > A^{(1)}$  there is no  $x_0$  which makes the locking condition for  $n=0$  fulfilled. For  $A > A^{(1)}$ , however, the condition (6.5) for  $n=1$  can be fulfilled and the system locks into the  $n=1$  region. At a certain value of  $A = A^{(2)}$  the condition (6.5) for  $n=1$  can not be fulfilled any more and the locked regime  $\langle \dot{x} \rangle = 2\Omega (n=2)$  cannot be reached for  $\Omega=1$ . Thus, the system cannot lock to the external signal and the voltage  $\langle \dot{x} \rangle$  shows oscillatory behavior as a function of the driving am-

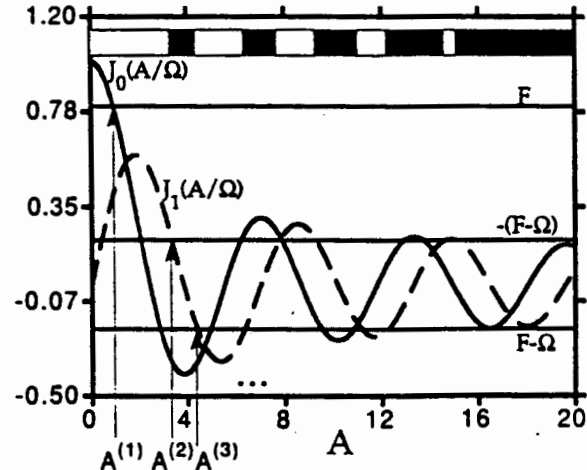


Fig. 7 The functions  $J_0(A/\Omega)$  (full line) and  $J_1(A/\Omega)$  (dashed line) are plotted together with the straight lines  $F$ ,  $F-\Omega$  and  $\Omega-F$ . The light regions of the stripe on top of the curves indicate phase locked regions

plitude. Due to the oscillatory behavior of the Bessel functions, the locking condition for  $n = 1$  can be fulfilled again in a number of intervals of larger  $A$ . It is obvious from Fig. 7 that the width of the locked intervals decrease for increasing values of the driving amplitude  $A$  until the Bessel functions, which decay asymptotically proportional to  $A^{-1/2}$ , are too small for locking. Note, that the agreement of the numerical values  $A^{(0)}$  (Fig. 6a) with those obtained from the theory becomes better for increasing driving amplitudes.

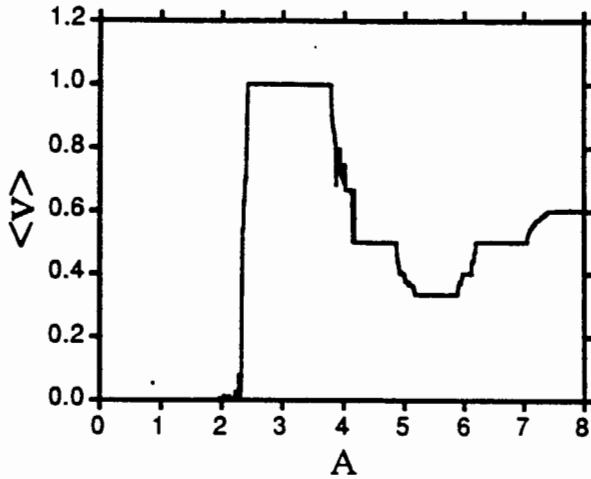


Fig. 8  
The dynamical current voltage characteristic with an inertia term (model (3.4)) is shown for  $F = 0.5$ ,  $\bar{Q} = 1$  and  $\gamma = 1$ .

The dynamical current-voltage characteristics for systems with inertia (the model 3.4)) is even more rich, since it allows also for subharmonic phase locking, i.e.

$$\langle v \rangle = \frac{m}{n} \Omega \quad m, n \in \mathbb{N}. \quad (6.7)$$

The numerical results for  $F = 0.5$ ,  $\bar{Q} = 1$  and  $\gamma = 1$  are shown in Fig. 8 for vanishing noise. The voltage  $\langle \dot{x} \rangle$  as a function of the driving amplitude shows besides the steps also regions with wild oscillations. These oscillations occur with chaotic solutions.

## 7. Conclusions

In this paper we have presented a concept for escape rates in periodically driven systems. For a periodic (multistable) potential we have derived explicit results for the escape rate as a function of the driving frequency and amplitude. The relations between rates, mobility and diffusion coefficients have been discussed as well as the role of boundary condi-

tions. In addition we have presented dynamical current-voltage characteristics, i.e.  $\langle \dot{x} \rangle$  as a function of the driving amplitude  $A$ . The observed rich dynamical behavior has been explained in terms of phase locking.

We are grateful for the financial support by the Stiftung Volkswagenwerk. We wish to thank Peter Talkner for helpful discussions on rate theory.

## References

- [1] In "Optical Bistability III", edited by H. M. Gibbs, P. Mandel, N. Peyghambarian and S. D. Smith, Springer-Verlag Berlin, Heidelberg, New-York, Tokyo.
- [2] For an overview, see A. Barone and G. Paterno, *Physics and Applications of the Josephson Effect*, John Wiley & Sons, New York 1982.
- [3] For an overview see P. Hänggi, P. Talkner, and M. Borkovec, *Rev. Mod. Phys.* **62**, 251 (1990).
- [4] K. H. Kramers, *Physica* **7**, 284 (1940).
- [5] See references in Ref. [3].
- [6] a) B. Carmeli and A. Nitzan, *Phys. Rev. A* **32**, 2435 (1985); b) H. M. Devoret, D. Esteve, J. M. Martinis, and J. Clarke, *Phys. Rev. B* **36**, 58 (1987); c) M. H. Devoret, J. M. Martinis, D. Esteve, and J. Clarke, *Phys. Rev. Lett.* **53**, 1260 (1984); d) A. L. Larkin and Yu. N. Ovchinnikov, *Low Temp. Phys.* **36**, 317 (1986); e) K. S. Chow and V. Ambegaokar, *Phys. Rev. B* **38**, 11168 (1988); f) S. Linkwitz, Ph. D. thesis, University of Stuttgart (1990); A. L. Gerasimov, *Phys. Lett. A* **135**, 29 (1989); A. L. Gerasimov, *J. Stat. Phys.* **60**, 485 (1990); J. F. Schonfeld, *Ann. Phys. (N.Y.)* **160**, 149–263 (1985).
- [7] P. Jung, *Z. Phys. B* **76**, 521 (1989).
- [8] L. Farkas, *Z. Phys. Chem. (Leipzig)* **125**, 236 (1927).
- [9] a) B. Caroli, C. Caroli, B. Roulet, and D. Saint-James, *Physica* **108 A**, 233 (1981); b) W. Weidlich and G. Haag, *Z. Phys. B* **39**, 81 (1980).
- [10] T. Zhou, F. Moss and P. Jung, *Phys. Rev. A* **42**, 3161 (1990).
- [11] P. Jung and P. Hänggi, *Europhys. Lett.* **8**, 505 (1989).
- [12] P. Jung and P. Hänggi, *Phys. Rev. A* **41**, 2977 (1990).
- [13] R. Kubo and Toda, "Statistical Physics II", Springer Series in Solid-State Sciences, eds. M. Cardona, P. Fulde, H.-J. Queisser, Springer Verlag, Berlin, Heidelberg, New-York.
- [14] R. L. Stratonovich, "Theory of Random Noise", Vol II, p. 254, Gordon & Breach, New York 1967.
- [15] M. Abramowitz and I. A. Stegun, *Handbook of Mathematical Functions*, Dover Publications, Inc., New York 1972.
- [16] R. L. Kautz, *J. Appl. Phys.* **52**, 3528 (1981).
- [17] a) A. J. Viterbi: "Principles of coherent communication", McGraw-Hill, New York 1966; b) W. C. Lindsay: "Synchronization Systems in Communication and Control", Prentice Hall, Englewood Cliffs, New York 1972.
- [18] W. Schleich, C.-S. Cha, and J. D. Cresser, *Phys. Rev. A* **29**, 230 (1984).
- [19] S. Shapiro, *Phys. Rev. Lett.* **11**, 80 (1963).
- [20] In large parts we follow the calculations in Ref. [16].

Presented at the Discussion Meeting of the Deutsche Bunsen-Gesellschaft für Physikalische Chemie "Rate Processes in Dissipative Systems: 50 Years after Kramers" in Tutzing, September 10–13, 1990 E 7501